



Spatiotemporal Analysis of Developing Brain Networks

Ping He^{1†}, Xiaohua Xu^{1*†}, Han Zhang^{2†}, Gang Li², Jingxin Nie³, Pew-Thian Yap² and Dinggang Shen^{2,4*}

¹ Department of Computer Science, Yangzhou University, Yangzhou, China, ² Department of Radiology and BRIC, University of North Carolina, Chapel Hill, NC, United States, ³ School of Psychology, South China Normal University, Guangzhou, China, ⁴ Department of Brain and Cognitive Engineering, Korea University, Seoul, South Korea

Recent advances in MRI have made it easier to collect data for studying human structural and functional connectivity networks. Computational methods can reveal complex spatiotemporal dynamics of the human developing brain. In this paper, we propose a Developmental Meta-network Decomposition (DMD) method to decompose a series of developmental networks into a set of Developmental Meta-networks (DMs), which reveal the underlying changes in connectivity over development. DMD circumvents the limitations of traditional static network decomposition methods by providing a novel exploratory approach to capture the spatiotemporal dynamics of developmental networks. We apply this method to structural correlation networks of cortical thickness across subjects at 3–20 years of age, and identify four DMs that smoothly evolve over three stages, i.e., 3–6, 7–12, and 13–20 years of age. We analyze and highlight the characteristic connections of each DM in relation to brain development.

Keywords: structural correlation networks, developmental networks, cortical thickness, developmental meta-network decomposition, non-negative matrix factorization

OPEN ACCESS

Edited by:

Arjen van Ooyen,
VU University Amsterdam,
Netherlands

Reviewed by:

Vince D. Calhoun,
University of New Mexico,
United States
Budhachandra Singh Khundrakpam,
McGill University, Canada

*Correspondence:

Xiaohua Xu
arterx@gmail.com
Dinggang Shen
dinggang_shen@med.unc.edu

[†]These authors have contributed
equally to this work.

Received: 18 April 2018

Accepted: 10 July 2018

Published: 31 July 2018

Citation:

He P, Xu X, Zhang H, Li G, Nie J,
Yap P-T and Shen D (2018)
Spatiotemporal Analysis of Developing
Brain Networks.
Front. Neuroinform. 12:48.
doi: 10.3389/fninf.2018.00048

1. INTRODUCTION

Understanding normal brain development is critical for basic developmental neuroscience. Recent advances in MRI have made it easier to collect data for studying human structural and functional connectivity networks. For example, the multi-site NIH MRI Study of Normal Brain Development has collected developmental structural MRI of over a thousand of children, ranging from infancy to young adulthood. The rich spatial and temporal information afforded in such datasets calls for sophisticated computational methods to capture the dynamic changes in brain connectivity during the course of development.

To date, most developmental studies are mainly focused on charting network characteristics, such as small-world properties, global efficiency, local efficiency, and etc. (Menon, 2013; Olde Dubbelink et al., 2013; Wu et al., 2013; Hadley et al., 2016). They treat the developmental networks as a group of static networks and compute their network characteristics independently. Alternatively, community detection algorithms are used to investigate the temporal evolution of modular organization (Mucha et al., 2009; Betzel and Bassett, 2017). The detected modules are recognized as sets of brain regions that perform specific cognitive functions.

To study temporal changes in brain connectivity, various matrix decomposition methods, especially principal component analysis (PCA), independent component analysis (ICA), and non-negative matrix factorization (NMF) have been applied to developmental structural and functional networks to identify the intrinsic components (Ghanbari et al., 2014; Sotiras et al., 2017)

or connectivity states (Leonardi et al., 2013; Calhoun et al., 2014; Miller et al., 2016). Compared with other matrix decomposition methods, NMF is featured with its non-negativity constraint imposed on the elements of the decomposed factor matrices. This constraint leads to a parts-based representation (Lee and Seung, 1999), thus making the decomposition results more interpretable. During brain development, brain connectivity may evolve through different stages. Accordingly, the intrinsic connectivity components, which we refer to as meta-networks, may also develop across different stages. In this paper, we call such evolving intrinsic component as *developmental meta-networks* (DMs) and propose an approach for Developmental Meta-network Decomposition (DMD). DMD decomposes the developmental networks into a set of temporally smooth DMs that capture the underlying connectivity patterns across developmental stages to adapt to the cognitive development. DMD not only automatically identifies the developmental stages and the number of DMs, but also uncovers the evolution of DMs. In this study, we apply DMD to *developmental networks* constructed based on inter-regional cortical thickness correlation across subjects for age spanning 3–20 years.

2. MATERIALS AND METHODS

2.1. Datasets and Construction of Blue Developmental Networks

This study uses the Pediatric MRI Data Repository¹ released by the NIH MRI Study of Normal Brain Development (Evans, 2006), which is a multi-site developmental study with the objective to collect developmental data for investigating brain maturation in connection with behavioural and cognitive development in normal populations (Evans, 2006; Waber et al., 2007). We adopt 951 scans from 445 subjects of 3 to 20 years of age (Figure S1). The age in years are obtained by subtracting the date of birth from the date of visit. Each subject is scanned in two or more MRI sessions over a five-to-six-year period.

For each participant, a three-dimensional sagittal T1-weighted image was acquired using a 1.5 T scanner with 1 mm isotropic resolution. Each image was skull stripped to remove non-cerebral tissues (Smith, 2002), corrected for intensity inhomogeneity, and segmented into gray matter (GM), white matter (WM), and cerebrospinal fluid (CSF) (Zhang et al., 2001). FSL 4.3 were used to perform brain extraction (BET) and tissue segmentation (FAST). To ensure the image processing quality, we visually checked the brain extraction and segmentation results for each subjects less than 5 years old. Different parameters were tried until the segmentation result were acceptable. Inner and outer cortical surfaces were reconstructed by a deformable surface method (Li et al., 2012). With the automated anatomical labelling (AAL) template (Tzourio-Mazoyer et al., 2002), each cortical surface was parcellated into 78 regions of interest (ROIs) (see Table S1) based on a non-linear hybrid volumetric/surface registration method (Liu et al., 2004).

Cortical thickness was measured between the reconstructed inner and outer cortical surfaces using the shortest distance in

the native space at each vertex (Liu et al., 2008). Regional cortical thickness was defined as the average thickness of all vertices within an ROI. We removed the effects of multiple confounding variables, including gender and overall mean cortical thickness, via linear regression analysis for each cortical region at each age (He et al., 2007). The regression residuals were taken as the corrected cortical thickness values.

The details of networks construction based on cortical thickness is described in Nie et al. (2013). An inter-regional cortical thickness correlation network was built for each time point by computing the pairwise Pearson's correlation coefficient of cortical properties across subjects. Take age 3 for example, there were 45 unique subjects, then each ROI was represented by a cortical thickness vector of length 45. By computing the Pearson's correlation coefficient between each pair of ROI vectors, we built a 78×78 inter-regional correlation network for age 3. We used the absolute values of the correlation matrices as in other studies (Khundrakpam et al., 2013). In the network matrix, a zero entry represents absence of connection, whereas a positive entry indicates the strength of pairwise inter-regional correlation. In this way, we obtained the developmental networks composed of eighteen 78×78 symmetric non-negative networks of 3–20 years of age (Figure S2).

2.2. Developmental Meta-Network Decomposition (DMD)

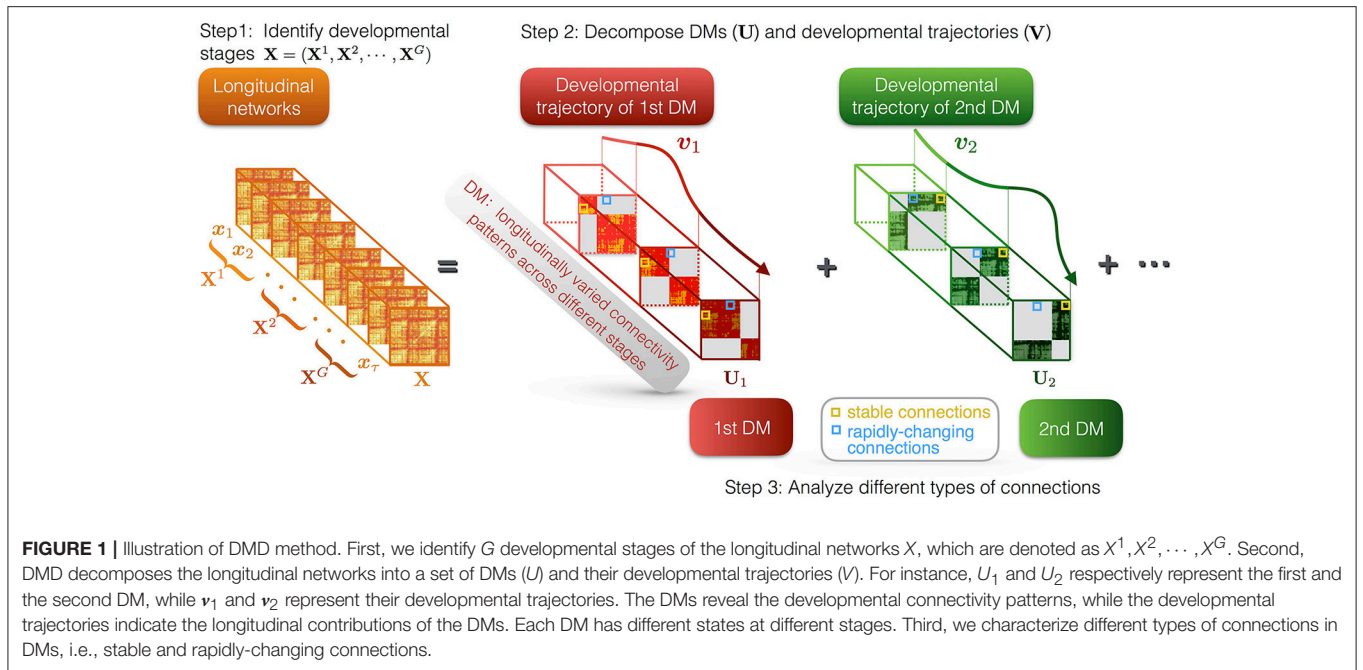
DMD method is composed of three parts (see Figure 1): (i) identifying the developmental stages of the developmental networks; (ii) decomposing the developmental networks into a set of DMs and their trajectories; (iii) characterization of the different types of connections in DMs, i.e., stable and rapidly-changing connections.

2.2.1. Identifying Developmental Stages

The evolution of DMs is essentially caused by the change of developmental networks across different developmental stages. An ideal partition of developmental stages satisfies that the networks in the same stage are close to each other, while the networks in different stages are significantly different from each other.

To achieve this aim, we use the method of consensus clustering (Ozdemir et al., 2015; Wu et al., 2015), which yields a stable and robust partition. We run the sensitive k-means clustering algorithm on the vectorized developmental brain networks with different numbers of clusters. For each number of clusters, we record the clustering results for 100 runs with randomized seeds, and use the criterion of *dispersion coefficient* to evaluate the consistency of the clustering results (Brunet et al., 2004). The larger the dispersion coefficient, the more consistent the clustering results. The optimal partition of developmental stages is the one that leads to the largest dispersion coefficient in the finest granularity. In another word, if there are multiple partitions leading to the same highest dispersion coefficient, we prefer the one that reveals the most detailed developmental stages of the age-related networks.

¹<https://pediatricmri.nih.gov/nihpd/info/index.html>



2.2.2. Developmental Meta-Network Decomposition

Let $\mathbf{X} = [\mathbf{x}_1 \ \mathbf{x}_2 \ \dots \ \mathbf{x}_\tau]$ be the developmental non-negative networks, where $\mathbf{x}_i \in \mathbb{R}_+^M$ represents the vectorized network at the i^{th} time point, M is the number of connections in each network (i.e., $78 \times 77/2$ in this study due to the symmetry of network), τ is the number of time points. Assume that the τ developmental networks consist of G developmental stages, let $\mathbf{X}^t = [\mathbf{x}_{i_1} \ \mathbf{x}_{i_2} \ \dots \ \mathbf{x}_{i_{n_t}}] \in \mathbb{R}^{M \times n_t} (\forall t \in [1, G])$ denote the t^{th} developmental stage, then \mathbf{X} can be reorganized as $\mathbf{X} = [\mathbf{X}^1 \ \mathbf{X}^2 \ \dots \ \mathbf{X}^G]$. Our aim is to decompose a set of DMs (denoted as \mathbf{U}) and their developmental trajectories (denoted as \mathbf{V}) from \mathbf{X} . Note that we allow each DM to evolve across different stages, instead of remaining unchanged through development.

We start from considering the decomposition of a single developmental stage \mathbf{X}^t . It is an observation of the t^{th} developmental stage that consists of two parts. One is the true developmental networks of the t^{th} stage ($\hat{\mathbf{X}}^t$), the other is the noise introduced during image acquisition, preprocessing and etc. To reduce the impact of noise, we perform decomposition on $\hat{\mathbf{X}}^t$ instead of observed \mathbf{X}^t . We assume that $\hat{\mathbf{X}}^t$ can be represented as a linear combination of p DMs at the t^{th} stage (\mathbf{U}^t), whose contributions are indicated by their trajectories (\mathbf{V}^t), i.e., $\hat{\mathbf{X}}^t = \mathbf{U}^t \mathbf{V}^{tT}$. The combined objective function of true data recovery and DM decomposition is given in Equation (1).

$$\begin{aligned} \min_{\hat{\mathbf{X}}^t} & \frac{1}{2} \|\mathbf{X}^t - \hat{\mathbf{X}}^t\|_F^2 + \lambda \|\hat{\mathbf{X}}^t\|_* \\ \text{s.t.} & \hat{\mathbf{X}}^t = \mathbf{U}^t \mathbf{V}^{tT}, \mathbf{U}^{tT} \mathbf{U}^t = \mathbf{I}, \mathbf{U}^t \geq 0, \mathbf{V}^t \geq 0 \end{aligned} \quad (1)$$

The first term in Equation (1) minimizes the difference between $\hat{\mathbf{X}}^t$ and \mathbf{X}^t , the second term penalizes the nuclear norm of $\hat{\mathbf{X}}^t$, which implies the number of DMs. The orthogonal constraint $\mathbf{U}^{tT} \mathbf{U}^t = \mathbf{I}$ avoids finding overlapped connectivity patterns.

Besides, the non-negativity constraints on \mathbf{U}^t and \mathbf{V}^t facilitate their neurobiological interpretation as DMs and developmental trajectories. To simplify the formulation, we replace $\hat{\mathbf{X}}^t$ with the product of \mathbf{U}^t and \mathbf{V}^{tT} in Equation (1) and have the following objective function.

$$\min_{\substack{\mathbf{U}^t, \mathbf{V}^t \geq 0 \\ \mathbf{U}^{tT} \mathbf{U}^t = \mathbf{I}}} \frac{1}{2} \|\mathbf{X}^t - \mathbf{U}^t \mathbf{V}^{tT}\|_F^2 + \lambda \|\mathbf{U}^t \mathbf{V}^{tT}\|_* \quad (2)$$

Next, we take all the developmental stages into consideration. According to existing neural network models, nervous systems can change smoothly by slowly changing connectivity patterns and strength (Enquist and Ghirlanda, 2005). Inspired by that, we define the overall objective function as the sum of all the single-stage objective function plus a cross-stage smoothness regularization term $\mathcal{R}(\mathbf{U}, \mathbf{V})$.

$$\min_{\substack{\mathbf{U}^t, \mathbf{V}^t \geq 0 \\ \mathbf{U}^{tT} \mathbf{U}^t = \mathbf{I}}} \sum_{t=1}^G \left(\frac{1}{2} \|\mathbf{X}^t - \mathbf{U}^t \mathbf{V}^{tT}\|_F^2 + \lambda \|\mathbf{U}^t \mathbf{V}^{tT}\|_* \right) + \mathcal{R}(\mathbf{U}, \mathbf{V}) \quad (3)$$

where

$$\mathcal{R}(\mathbf{U}, \mathbf{V}) \stackrel{\text{def}}{=} \frac{\alpha}{4} \sum_{k,l=1}^G \mathbf{W}_{\mathbf{U}}(k,l) \|\mathbf{U}^k - \mathbf{U}^l\|_F^2 + \frac{\beta}{4} \sum_{i,j=1}^{\tau} \mathbf{W}_{\mathbf{V}}(i,j) \|\mathbf{v}_i - \mathbf{v}_j\|^2 \quad (4)$$

In Equation (4), the first term of $\mathcal{R}(\mathbf{U}, \mathbf{V})$ measures the temporal smoothness of \mathbf{U} across different states, where $\mathbf{W}_{\mathbf{U}}(k,l)$ indicates the adjacency between the k^{th} and l^{th} developmental stages. The second term of $\mathcal{R}(\mathbf{U}, \mathbf{V})$ measures the temporal smoothness of \mathbf{V} across different time points, where $\mathbf{W}_{\mathbf{V}}(i,j)$ measures the adjacency between the i^{th} and j^{th} time points.

Since it has been proved that minimizing the nuclear norm of the product of two non-negative matrices is equivalent to minimizing half of their squared Frobenius norm (Srebro and Shraibman, 2005), we can replace the nuclear norm $\|\mathbf{U}^t \mathbf{V}^{tT}\|_*$ in Equation (3) with $\frac{1}{2}(\|\mathbf{U}^t\|_F^2 + \|\mathbf{V}^t\|_F^2)$. Besides, notice that $\|\mathbf{U}^t\|_F^2 = \text{tr}(\mathbf{U}^{tT} \mathbf{U}^t) = p$ and $\sum_{t=1}^G \|\mathbf{V}^t\|_F^2 = \|\mathbf{V}\|_F^2$, we can rewrite the objective function in the following form.

$$\mathcal{J} = \min_{\substack{\mathbf{U}^t, \mathbf{V}^t \geq 0 \\ \mathbf{U}^{tT} \mathbf{U}^t = \mathbf{I}}} \sum_{t=1}^G \frac{1}{2} \|\mathbf{X}^t - \mathbf{U}^t \mathbf{V}^{tT}\|_F^2 + \frac{1}{2} \lambda \|\mathbf{V}\|_F^2 + \mathcal{R}(\mathbf{U}, \mathbf{V}) \quad (5)$$

Therefore, we obtain the multiplicative updating rules for \mathbf{U}^t and \mathbf{V} as follows.

$$\mathbf{U}^t \leftarrow \mathbf{U}^t \odot \frac{\left[\mathbf{X}^t \mathbf{V}^t + \alpha \sum_{k=1}^G \mathbf{W}_{\mathbf{U}}(t, k) \mathbf{U}^k \right]}{\left[\mathbf{U}^t \mathbf{V}^{tT} \mathbf{X}^t \mathbf{V}^t + \alpha \sum_{k=1}^G \mathbf{W}_{\mathbf{U}}(t, k) \mathbf{U}^t \mathbf{U}^{kT} \mathbf{U}^k \right]} \quad (6)$$

$$\mathbf{V} \leftarrow \mathbf{V} \odot \frac{\left[\sum_{t=1}^G \mathbf{H}^t \mathbf{X}^{tT} \mathbf{U}^t + \beta \mathbf{W}_{\mathbf{V}} \mathbf{V} \right]}{\left[\sum_{t=1}^G \mathbf{H}^t \mathbf{H}^{tT} \mathbf{V} \mathbf{U}^{tT} \mathbf{U}^t + \lambda \mathbf{V} + \beta \mathbf{D}_{\mathbf{V}} \mathbf{V} \right]} \quad (7)$$

where $\mathbf{H}^t \stackrel{\text{def}}{=} (\mathbf{e}_{i_1}, \mathbf{e}_{i_2}, \dots, \mathbf{e}_{i_{n_t}})$ is the mask matrix of \mathbf{V}^t satisfying $\mathbf{V}^t = \mathbf{H}^{tT} \mathbf{V}$, \mathbf{e}_{i_j} is a 0/1 vector with the only positive element at the i_j -th index, $\mathbf{D}_{\mathbf{V}}$ is the degree matrix of $\mathbf{W}_{\mathbf{V}}$, \odot and the bar respectively denote element-wise product and division. The convergence proof of the multiplicative updating rules can be referred to that of non-negative matrix decomposition (Lee and Seung, 1999). To avoid local minimum, we adopt an initialization strategy on \mathbf{U} and \mathbf{V} similar to that of k -means algorithm, i.e., repeating multiple (100) times with random initializations and choosing the one with the least cost. The empirical convergence of DMD method is shown on Figure S3. The method is robust to a wide range of the regularization parameters (Figure S4).

The number of DMs is determined by maximizing Minimal Trajectory Distance (MTD), which computes the minimal distance between pairwise developmental trajectories. The larger MTD, the more separable the developmental trajectories, the more distinct and biologically significant the corresponding DMs.

2.2.3. Characterizing Different Types of Connections in DMs

On the basis of developmental meta-network decomposition, we characterize two types of connections in DMs, i.e., *stable connections* and *rapidly-changing connections*, for analysis.

The *stable connections* constitute the “bones” of DMs that keep unchanged through development, while their contributions in the developmental networks are indicated by the developmental trajectories. We select the stable connections with the least normalized divergence (e.g., top 2%) for each DM, and exclude

those insignificant connections with average strength ($\overline{\mathbf{U}}_r$) less than a threshold (δ_r). Take the r^{th} DM (denoted as \mathbf{U}_r) for example,

$$\Omega(\mathbf{U}_r) = \frac{\text{div}(\mathbf{U}_r)}{\overline{\mathbf{U}}_r} = \frac{\left[\sum_{k,t=1}^G |\mathbf{u}_r^k - \mathbf{u}_r^t| \right]}{\left[\frac{1}{G} \sum_{t=1}^G \mathbf{u}_r^t \right]} \quad (8)$$

$\Omega(\mathbf{U}_r)$ in Equation (8) computes the normalized divergence of the connections in the r^{th} DM, where \mathbf{u}_r^t represents the t^{th} state of \mathbf{U}_r . The threshold δ_r is adaptively determined by the quadratic mean (or root mean square value) of \mathbf{U}_r , where GM is the number of connections in \mathbf{U}_r .

$$\delta_r = \sqrt{\frac{\|\mathbf{U}_r\|_F^2}{GM}} \quad (9)$$

The *rapidly-changing connections* highlight the most important changes in the inter-regional coordination during brain development. We characterize this type of connections by taking into account of both DMs and their developmental trajectories. For each DM, we select the most significantly increased and decreased connections across adjacent stages by computing $\Delta \mathbf{u}_r^t = (\mathbf{u}_r^{t+1} - \mathbf{u}_r^t)$. Meanwhile, we calculate the stage contributions of each DM by averaging its within-stage trajectory, i.e., $\bar{v}_r^t = \text{mean}(\mathbf{v}_r^t)$. The rapidly-changing connections are the ones with the same direction of change (\uparrow or \downarrow) in both DMs ($\Delta \mathbf{u}_r^t$) and their stage contributions across adjacent stages ($\Delta \bar{v}_r^t = \bar{v}_r^{t+1} - \bar{v}_r^t$), thus indicating the changes in the developmental networks.

2.2.4. Reproducibility

To evaluate the reproducibility of DMD method, we use a split-half strategy, i.e., dividing the developmental networks into two halves with odd-numbered ages (3, 5, \dots , 19) and even-numbered ages (4, 6, \dots , 20). The reproducibility is quantified by computing similarity between the corresponding DMs (or developmental trajectories), which are independently decomposed from the two splits and matched using the Hungarian algorithm (Kuhn, 2005). We use the cosine similarity to measure the similarity between the matched DMs (or trajectories), as did in Lange et al. (2004). Since the two splits of developmental networks have a temporal gap of one year, cosine similarity is especially advantageous in the evaluation of trajectory reproducibility, because it is a judgment of orientation instead of magnitude.

3. RESULTS

We apply DMD method to the developmental structural correlation networks and obtain four DMs, which evolve across three identified developmental stages, including ages 3–6, 7–12, and 13–20, respectively (Figure S5). For the identification of developmental stages and the DM number, please refer to the subsection *Parameter Influence*.

3.1. Stable and Rapidly-Changing Connections of DMs

We extract the stable connections of the four DMs (**Figure 2A**), whose contributions in the development are indicated by the developmental trajectories (**Figure 2B**). In the first DM, the stable connections exhibit an *indirect connection pattern*, which looks like “ ∞ ,” between the prefrontal and occipital areas through interlaying temporal regions. The trajectory of the first DM shows that the *indirect connection pattern* decreases quickly at first but then slows down after the age of 13. In comparison, the stable connections of the second and third DMs are characterized with the *long direct connections* between the prefrontal and occipital areas. The trajectories of these *direct connections*, after going through ups and downs, reach higher values at the age of 20 than at the age of 3 years. Combined together, they indicate the gradual replacement of the *indirect connection pattern* by the *direct connection pattern* from age 3 to 20 years. This is consistent with the development of functional network architecture, where regional interactions change from being predominantly anatomically local in children to interactions spanning longer cortical distances in young adults (Vogel et al., 2010). Besides, the stable connections of the fourth DM are composed of short-range connections and homologous connections between homotopic regions. Similar connections were also found as the most common and robust connections among different individuals (Hermundstad et al., 2013).

On the other side, we study the rapidly-changing connections of DMs. Since the fourth DM is the most stable one with almost negligible change of connection strength (**Figure 3A**), we will focus on the rapidly-changing connections of the other three DMs. During the transition from the first developmental stage (ages 3–6) to the second (ages 7–12), the first DM shows both significantly decreased connection strength and stage contribution (**Figures 3A,B**). Its rapidly-weakened connections indicate the decrease of the frontal part of the *indirect connection pattern* (∞) between the prefrontal and temporal regions (**Figure 3C**). Meanwhile, the second DM shows both significantly increased connection strength and stage contribution. Its rapidly-enhanced connections highlight three hubs, ACG.R (right anterior cingulate gyrus) and bilateral MCG (middle cingulate gyrus). Since those regions are involved in emotion formation and processing (Bush et al., 2000; Hadland et al., 2003), their enhanced connections may indicate the *emotional development* after 7 years old. In fact, 7 years of age is indeed the critical time point when impulses of primitive emotion are subjugated to reason and internalized social control (Cole et al., 1994; Pierre Philippot, 2013).

In the transition from the second developmental stage (ages 7–12) to the third (ages 13–20), the first DM is still featured with decreased connection strength and decreased stage contribution (**Figure 3D**). Its rapidly-weakened connections demonstrate the continued decrease of the frontal part of the

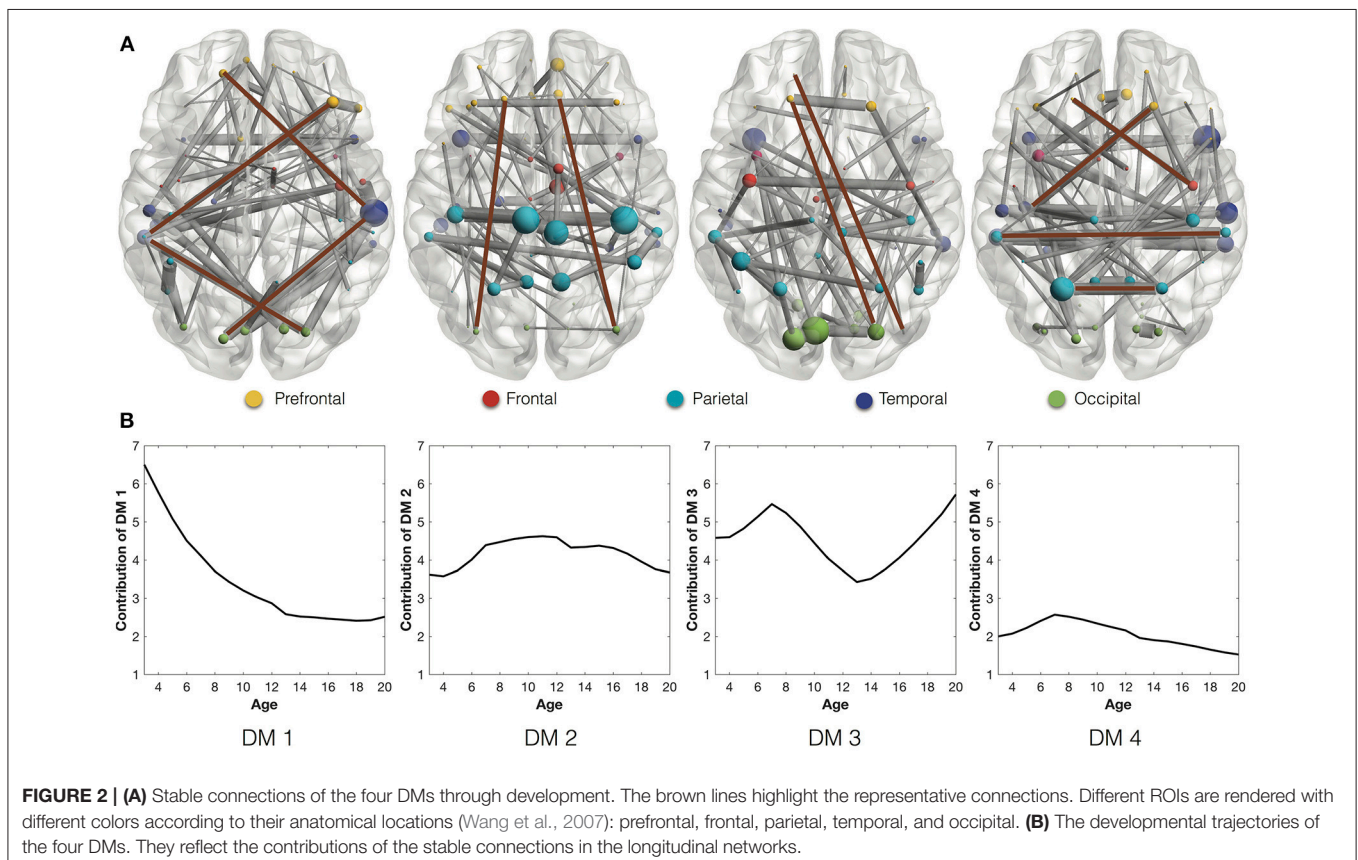
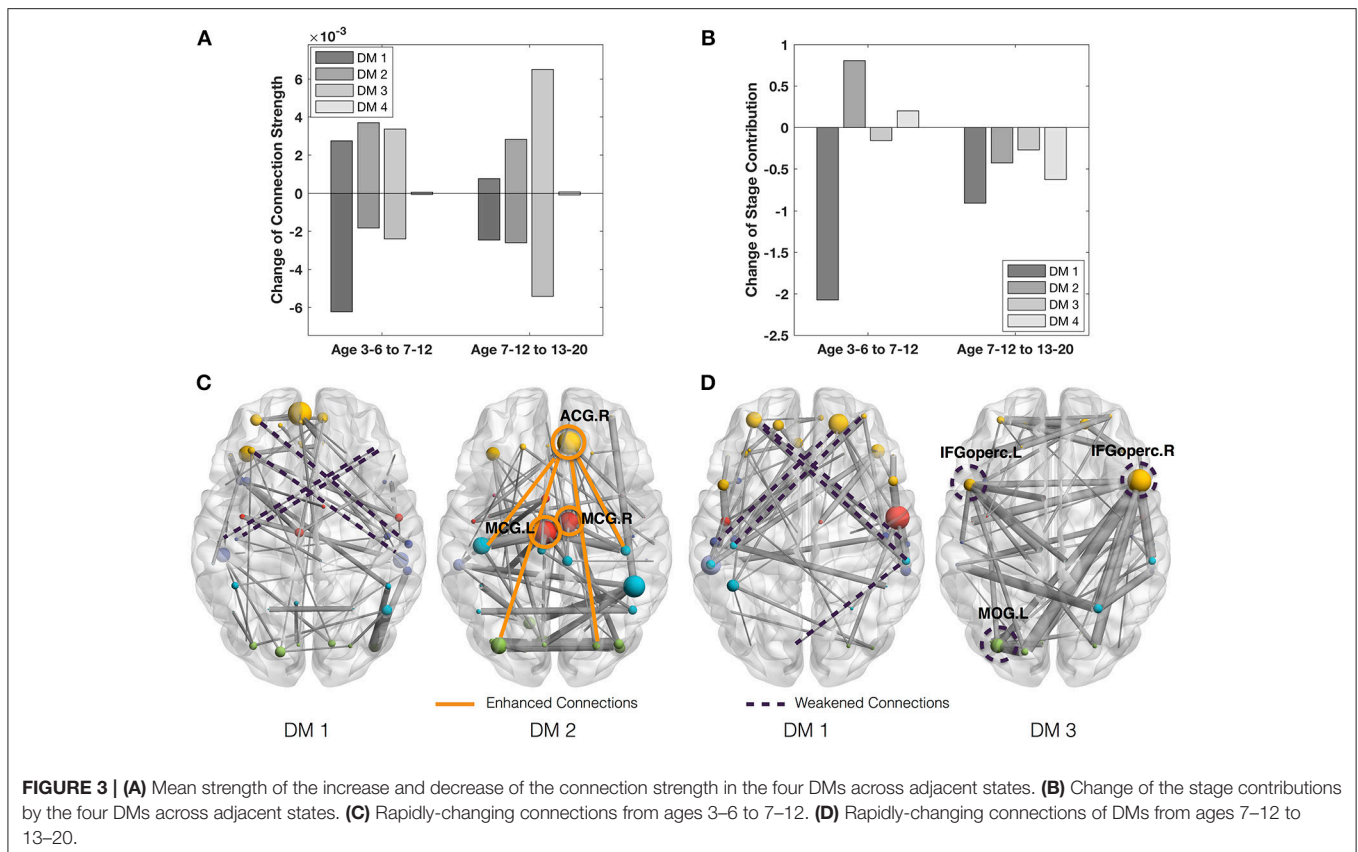


FIGURE 2 | (A) Stable connections of the four DMs through development. The brown lines highlight the representative connections. Different ROIs are rendered with different colors according to their anatomical locations (Wang et al., 2007): prefrontal, frontal, parietal, temporal, and occipital. **(B)** The developmental trajectories of the four DMs. They reflect the contributions of the stable connections in the longitudinal networks.



indirect connection pattern between the prefrontal and temporal regions. Meanwhile, the third DM shows the most significantly decreased connection strength and moderately decreased stage contribution. Its rapidly-weakened connections highlight three inter-connected hubs, including bilateral IFGoperc (opercular inferior frontal gyri) and MOG.L (left middle occipital gyrus). Since IFGoperc.L play a role in processing word phonology (Shaywitz et al., 1995) and IFGoperc.R is involved in visual and auditory spelling tasks (Booth et al., 2003), their weakened connections may indicate the *decline of language development* since 13 years old. This finding is consistent with Lenneberg's classic hypothesis about the age limitation (12–13 years) in the first language acquisition (Lenneberg, 1967) as well as Collier's studies that the first language acquisition is largely completed by the age of 12 (Collier, 1987, 1989).

To summarize, we have three major findings from the characteristic connections of DMs, which are validated in Figure S6.

1. The *indirect connections* between the prefrontal and occipital regions gradually, to some extent, get replaced by the *direct connections* from 3 to 20 years of age.
2. The connections with the *emotion-related* regions (ACG.R and bilateral MCG) are significantly *increased* from 6 to 12 years of age.
3. The connections with the *language-related* regions (IFGoperc.L and IFGoperc.R) are significantly *decreased* from 13 to 20 years of age.

3.2. Parameter Influence

We first study the influence of stage number on the quality of the developmental stage partition (**Figure 4**). With the increase of stage number (G), the developmental stage partition at first keeps very robust in consensus clustering, but then exhibits growing instability when G becomes larger than 3. Therefore, in this study we choose the most robust developmental stage partition in the finest granularity, i.e., three stages including 3–6, 7–12, and 13–20 years of age. Note that although we do not utilize any temporal information, the developmental stage partitions still group the networks at adjacent time points together, indicating the smooth change of the developmental networks.

Next we show the influence of the DM number on the separability of developmental trajectories (**Figure 5**). With the increase of the DM number, MTD at first gradually increases because more and more distinct DMs are separated from the average pattern (underfitting). When the DM number grows larger than four, MTD sharply drops off, then rises to a local maximum at seven DMs, which might indicate the existence of DM sub-patterns. After that, MTD continues to decline and finally reaches a very low value, because more and more insignificant DMs are separated from the dominant ones (overfitting). Therefore, in this study we choose four DMs that leads to the most distinct DMs with the most separable developmental trajectories.

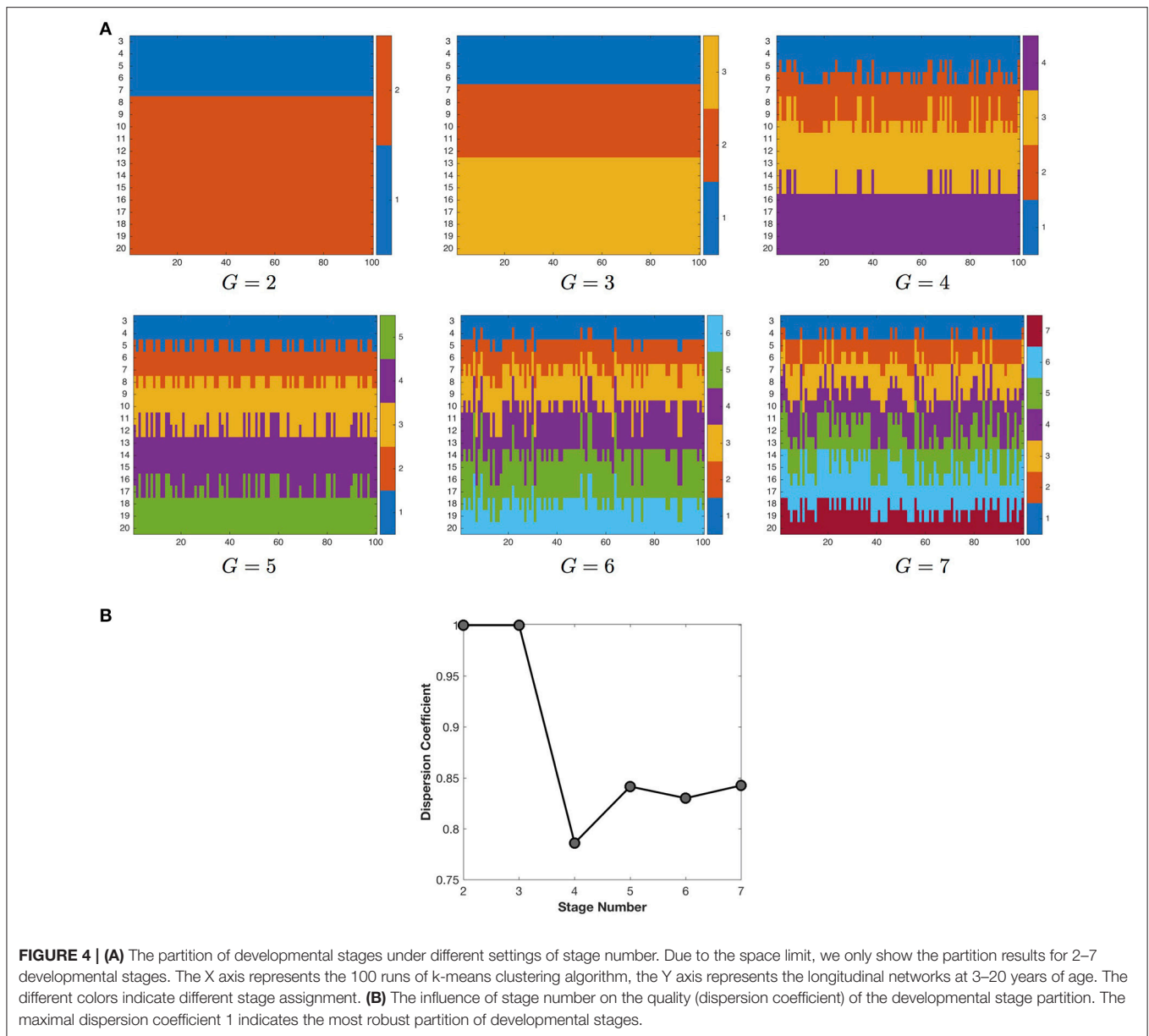


FIGURE 4 | (A) The partition of developmental stages under different settings of stage number. Due to the space limit, we only show the partition results for 2–7 developmental stages. The X axis represents the 100 runs of k-means clustering algorithm, the Y axis represents the longitudinal networks at 3–20 years of age. The different colors indicate different stage assignment. **(B)** The influence of stage number on the quality (dispersion coefficient) of the developmental stage partition. The maximal dispersion coefficient 1 indicates the most robust partition of developmental stages.

3.3. DMD Reproducibility

We also examine the reproducibility of DMs and their developmental trajectories under different settings of DM number (Figure 6). The reproducibility of DMs reaches maximum at the DM number of four (Figure 6A), while the reproducibility of developmental trajectories get slightly decreased with the increase of the DM number (Figure 6B). Therefore, in this study it is a reasonable choice to set the DM number as four.

4. DISCUSSION

We propose the DMD method to decompose developmental networks into a set of DMs and their developmental trajectories.

One important advantage of our approach is that it goes beyond current static network decomposition strategies to capture dynamic temporal patterns of developmental networks. Moreover, it automatically identifies the partition of developmental stages as well as the number of DMs. Our analysis of normal developmental brain networks shows that the decomposed DMs contain not only stable connections but also rapidly-changing connections. Capturing variability in the connectivity patterns via DMs moves us closer to the clinic of the future.

DMD helps to find significant underlying changes in connectivity over development. For instance, the rapidly-changing connections of DMs reveal that (1) the connections with the emotion-related regions (ACG.R and bilateral MCG) are significantly increased after 7 years of age, and (2)

the connections with the language-related regions (bilateral IFGoperc) are significantly decreased after 13 years of age. These findings are consistent with the existing behavioral studies that emotion control gets enhanced at the age of 7 years (Cole et al., 1994; Pierre Philippot, 2013) and the first language acquisition is largely completed by the age of 12 years (Lenneberg, 1967; Collier, 1987, 1989). Compared with previous studies, DMD provides more connectome details for the development neuroscience community.

DMD has many other applications. In the clinical domain, DMs allow in-depth comparison between normal and abnormal developmental networks, which are usually related to a certain type of disease. We can apply the normal DMs, which are

decomposed from the normal developmental networks, to the abnormal developmental networks and obtain its abnormal developmental trajectories. By comparing the *normal* and *abnormal* developmental trajectories under the same DMs, we are able to identify when and how the abnormal trajectories deviate from the normal ones, thus providing insights into the underlying mechanism of the disease. For example, in this study the first three DMs show that the *indirect connections* between the prefrontal and occipital areas gradually get replaced by the *direct connections* with the growth of age. This indicates the increase of functional efficiency in the normal brain development (Achard and Bullmore, 2007; Vogel et al., 2010; Bullmore and Sporns, 2012), because direct neural connections are generally believed to use less time for signal transmission than the polysynaptic connections (Grossenbacher, 2001). Hence, if the abnormal trajectories of the first three DMs exhibit different trends from the normal ones, it implies the correlation between the disease and the functional efficiency development.

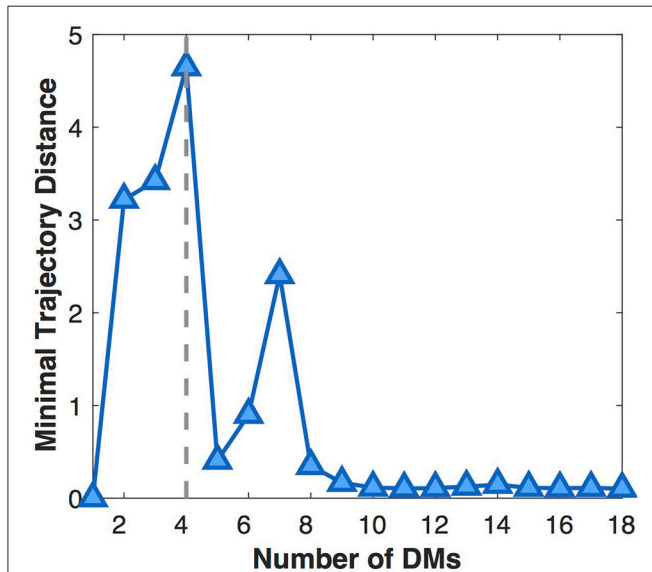


FIGURE 5 | Influence of the DM number on the separability of developmental trajectories (MTD). The larger the MTD value, the more separable the developmental trajectories.

5. LIMITATIONS AND FUTURE WORK

The current DMD method can only be applied to cross-sectional developmental networks, hence fail to fully utilize the longitudinal information of subjects. In our future work, we plan to extend the DMD method for early diagnosis of developmental disease of single subjects. This requires the application of DMD to within-subject, instead of across-subject, longitudinal networks. Although the data are progressively easier to collect based on Diffusion Tensor Imaging (DTI) or Functional MRI (fMRI), the main challenge lies in that different sets of DMs will be derived from different within-subject longitudinal networks. Therefore, it is necessary to extend DMD to decompose a representative set of DMs from multiple within-subject longitudinal networks. Then the representative set of DMs can be applied to single subjects for early disease diagnosis. We believe that DMD method will ultimately pave the way to much more refined representation and understanding of brain

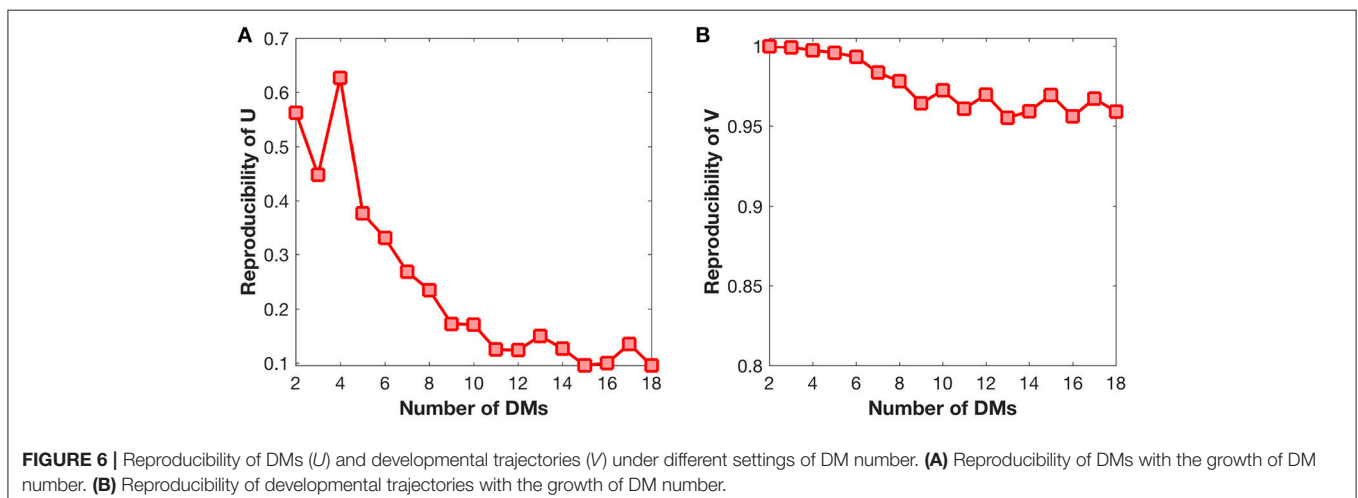


FIGURE 6 | Reproducibility of DMs (U) and developmental trajectories (V) under different settings of DM number. **(A)** Reproducibility of DMs with the growth of DM number. **(B)** Reproducibility of developmental trajectories with the growth of DM number.

network development, diseases, and other longitudinal biological phenomena.

ETHICS STATEMENT

This study was carried out in accordance with the recommendations of Name of Guidelines, Name of Committee with written informed consent from all subjects. All subjects gave written informed consent in accordance with the Declaration of Helsinki. The protocol was approved by the Name of Committee.

AUTHOR CONTRIBUTIONS

PH contributed to designing and analyzing the experiments, summarizing and visualizing the results, and writing the manuscript. XX contributed to developing and implementing the method, visualizing and analyzing the results. HZ, GL, and P-TY contributed to the critical revision of the manuscript and the discussion of the work. JN contributed to preparing the data and revising the manuscript. DS contributed to directing the whole project.

FUNDING

This work was supported in part by the Chinese National Natural Science Foundation under Grant Nos. 61402395, 61502412, 61379066, and 61300151, Natural Science Foundation of Jiangsu Province under contracts BK20151314, BK20140492, and BK20150459, Jiangsu Overseas Research and Training

Program for University Prominent Young and Middle-aged Teachers and Presidents, Jiangsu Government Scholarship for Overseas Studies. This work was also supported in part by National Institutes of Health grant MH100217, MH107815, MH108914.

ACKNOWLEDGMENTS

Data used in the preparation of this article were obtained from the Pediatric MRI Data Repository created by the NIH MRI Study of Normal Brain Development. This is a multi-site, longitudinal study of typically developing children, from ages newborn through young adulthood, conducted by the Brain Development Cooperative Group and supported by the National Institute of Child Health and Human Development, the National Institute on Drug Abuse, the National Institute of Mental Health, and the National Institute of Neurological Disorders and Stroke (Contract #s N01-HD02-3343, N01-MH9-0002, and N01-NS-9-2314, -2315, -2316, -2317, -2319, and -2320). A listing of the participating sites and a complete listing of the study investigators can be found at http://www.bic.mni.mcgill.ca/nihpd/info/participating_centers.html. This manuscript reflects the views of the authors and may not reflect the opinions or views of the NIH.

SUPPLEMENTARY MATERIAL

The Supplementary Material for this article can be found online at: <https://www.frontiersin.org/articles/10.3389/fninf.2018.00048/full#supplementary-material>

REFERENCES

- Achard, S., and Bullmore, E. (2007). Efficiency and cost of economical brain functional networks. *PLoS Comput. Biol.* 3:e17. doi: 10.1371/journal.pcbi.0030017
- Betzel, R. F., and Bassett, D. S. (2017). Multi-scale brain networks. *Neuroimage* 160, 73–83. doi: 10.1016/j.neuroimage.2016.11.006
- Booth, J. R., Burman, D. D., Meyer, J. R., Gitelman, D. R., Parrish, T. B., and Mesulam, M. M. (2003). Relation between brain activation and lexical performance. *Hum. Brain Mapp.* 19, 155–169. doi: 10.1002/hbm.10111
- Brunet, J. P., Tamayo, P., Golub, T. R., and Mesirov, J. P. (2004). Metagenes and molecular pattern discovery using matrix factorization. *Proc. Natl. Acad. Sci. U.S.A.* 101, 4164–4169. doi: 10.1073/pnas.0308531101
- Bullmore, E., and Sporns, O. (2012). The economy of brain network organization. *Nat. Rev. Neurosci.* 13, 336–349. doi: 10.1038/nrn3214
- Bush, G., Luu, P., and Posner, M. I. (2000). Cognitive and emotional influences in anterior cingulate cortex. *Trends Cogn. Sci.* 4, 215–222. doi: 10.1016/S1364-6613(00)01483-2
- Calhoun, V. D., Miller, R., Pearlson, G., and Adal, T. (2014). The chronectome: time-varying connectivity networks as the next frontier in fmri data discovery. *Neuron* 84, 262–274. doi: 10.1016/j.neuron.2014.10.015
- Cole, P. M., Michel, M. K., and Teti, L. O. (1994). The development of emotion regulation and dysregulation: a clinical perspective. *Monogr. Soc. Res. Child Dev.* 59, 73–100. doi: 10.2307/1166139
- Collier, V. P. (1987). The effect of age on acquisition of a second language for school. *Acad. Achiev.* 3:8.
- Collier, V. P. (1989). How long? A synthesis of research on academic achievement in a second language. *Tesol Q.* 23, 509–531. doi: 10.2307/3586923
- Enquist, M. and Ghirlanda, S. (2005). *Neural Networks and Animal Behavior*. Princeton, NJ: Princeton University Press.
- Evans, A. (2006). The NIH MRI study of normal brain development. *Neuroimage* 30, 184–202. doi: 10.1016/j.neuroimage.2005.09.068
- Ghanbari, Y., Smith, A. R., Schultz, R. T., and Verma, R. (2014). Identifying group discriminative and age regressive sub-networks from DTI-based connectivity via a unified framework of non-negative matrix factorization and graph embedding. *Med. Image Anal.* 18, 1337–1348. doi: 10.1016/j.media.2014.06.006
- Grossenbacher, P. G. (2001). *Finding Consciousness in the Brain*. Amsterdam: John Benjamins Publishing Company.
- Hadland, K. A., Rushworth, M. F. S., Gaffan, D., and Passingham, R. E. (2003). The effect of cingulate lesions on social behaviour and emotion. *Neuropsychologia* 41, 919–931. doi: 10.1016/S0028-3932(02)00325-1
- Hadley, J. A., Kraguljac, N. V., White, D. M., Ver Hoef, L., Tabora, J., and Lahti, A. C. (2016). Change in brain network topology as a function of treatment response in schizophrenia: a longitudinal resting-state fMRI study using graph theory. *NPJ Schizophrenia* 2:16014. doi: 10.1038/npschz.2016.14
- He, Y., Chen, Z. J., and Evans, A. C. (2007). Small-world anatomical networks in the human brain revealed by cortical thickness from MRI. *Cereb. Cortex* 17, 2407–2419. doi: 10.1093/cercor/bhl149
- Hermundstad, A. M., Bassett, D. S., Brown, K. S., Aminoff, E. M., Clewett, D., Freeman, S., et al. (2013). Structural foundations of resting-state and task-based functional connectivity in the human brain. *Proc. Natl. Acad. Sci. U.S.A.* 110, 6169–6174. doi: 10.1073/pnas.1219562110

- Khundrakpam, B. S., Reid, A., Brauer, J., Carbonell, F., Lewis, J., Ameis, S., et al. (2013). Developmental changes in organization of structural brain networks. *Cereb. Cortex* 23, 2072–2085. doi: 10.1093/cercor/bhs187
- Kuhn, H. W. (2005). The hungarian method for the assignment problem. *Naval Res. Logist.* 52, 7–21. doi: 10.1002/nav.20053
- Lange, T., Roth, V., Braun, M. L., and Buhmann, J. M. (2004). Stability-based validation of clustering solutions. *Neural Comput.* 16, 1299–1323. doi: 10.1162/089976604773717621
- Lee, D., and Seung, H. (1999). Learning the parts of objects by non-negative matrix factorization. *Nature* 401, 788–791. doi: 10.1038/44565
- Lenneberg, E. (1967). *Biological Foundations of Language*. Hoboken, NJ: Wiley.
- Leonardi, N., Richiardi, J., Gschwind, M., Simioni, S., Annoni, J. M., Schlupe, M., et al. (2013). Principal components of functional connectivity: a new approach to study dynamic brain connectivity during rest. *Neuroimage* 83, 937–950. doi: 10.1016/j.neuroimage.2013.07.019
- Li, G., Nie, J., and Shen, D. (2012). Consistent reconstruction of cortical surfaces from longitudinal brain MR images. *Neuroimage* 59, 3805–3820. doi: 10.1016/j.neuroimage.2011.11.012
- Liu, T., Nie, J., Tarokh, A., Guo, L., and Wong, S. T. (2008). Reconstruction of central cortical surface from brain MRI images: method and application. *Neuroimage* 40, 991–1002. doi: 10.1016/j.neuroimage.2007.12.027
- Liu, T., Shen, D., and Davatzikos, C. (2004). Deformable registration of cortical structures via hybrid volumetric and surface warping. *Neuroimage* 22, 1790–1801. doi: 10.1016/j.neuroimage.2004.04.020
- Menon, V. (2013). Developmental pathways to functional brain networks: emerging principles. *Trends Cogn. Sci.* 17, 627–640. doi: 10.1016/j.tics.2013.09.015
- Miller, R. L., Yaesoubi, M., Turner, J. A., Mathalon, D., Preda, A., Pearlson, G., et al. (2016). Higher dimensional meta-state analysis reveals reduced resting fmri connectivity dynamism in schizophrenia patients. *PLoS ONE* 11:e0149849. doi: 10.1371/journal.pone.0149849
- Mucha, P. J., Richardson, T., Macon, K., Porter, M. A., and Onnela, J. P. (2009). Community structure in time-dependent, multiscale, and multiplex networks. *Science* 328, 876–878. doi: 10.1126/science.1184819
- Nie, J., Li, G., and Shen, D. (2013). Development of cortical anatomical properties from early childhood to early adulthood. *Neuroimage* 76, 216–224. doi: 10.1016/j.neuroimage.2013.03.021
- Olde Dubbelink, K. T., Hillebrand, A., Stoffers, D., Deijen, J. B., Twisk, J. W., Stam, C. J., et al. (2013). Disrupted brain network topology in Parkinson's disease: a longitudinal magnetoencephalography study. *Brain* 137, 197–207. doi: 10.1093/brain/awt316
- Ozdemir, A., Bolaños, M., Bernat, E., and Aviyente, S. (2015). Hierarchical spectral consensus clustering for group analysis of functional brain networks. *IEEE Trans. Biomed. Eng.* 62, 2158–2169. doi: 10.1109/TBME.2015.2415733
- Pierre Philpott, R. S. F. (2013). *The Regulation of Emotion*. London: Psychology Press.
- Shaywitz, B. A., Shaywitz, S. E., Pugh, K. R., Constable, R. T., Skudlarski, P., Fulbright, R. K., et al. (1995). Sex differences in the functional organization of the brain for language. *Nature* 373, 607–609. doi: 10.1038/373607a0
- Smith, S. M. (2002). Fast robust automated brain extraction. *Hum Brain Mapp.* 17, 143–155. doi: 10.1002/hbm.10062
- Sotiras, A., Toledo, J. B., Gur, R. E., Gur, R. C., Satterthwaite, T. D., and Davatzikos, C. (2017). Patterns of coordinated cortical remodeling during adolescence and their associations with functional specialization and evolutionary expansion. *Proc. Natl. Acad. Sci. U.S.A.* 114, 3527–3532. doi: 10.1073/pnas.1620928114
- Srebro, N., and Shraibman, A. (2005). “Rank, trace-norm and max-norm,” in *Conference on Learning Theory* (Bertinoro: Springer), 545–560. doi: 10.1007/11503415_37
- Tzourio-Mazoyer, N., Landeau, B., Papathanassiou, D., Crivello, F., Etard, O., Delcroix, N., et al. (2002). Automated anatomical labeling of activations in spm using a macroscopic anatomical parcellation of the MNI MRI single-subject brain. *Neuroimage* 15, 273–289. doi: 10.1006/nimg.2001.0978
- Vogel, A. C., Power, J. D., Petersen, S. E., and Schlaggar, B. L. (2010). Development of the brain's functional network architecture. *Neuropsychol. Rev.* 20, 362–375. doi: 10.1007/s11065-010-9145-7
- Waber, D. P., De Moor, C., Forbes, P. W., Almlie, C. R., Botteron, K. N., Leonard, G., et al. (2007). The NIH MRI study of normal brain development: performance of a population based sample of healthy children aged 6 to 18 years on a neuropsychological battery. *J. Int. Neuropsychol. Soc. Image* 13, 729–746. doi: 10.1017/S1355617707070841
- Wang, K., Liang, M., Wang, L., Tian, L., Zhang, X., Li, K., et al. (2007). Altered functional connectivity in early Alzheimer's disease: a resting-state fMRI study. *Hum. Brain Mapp.* 28, 967–978. doi: 10.1002/hbm.20324
- Wu, J., Liu, H., Xiong, H., Cao, J., and Chen, J. (2015). K-means-based consensus clustering: a unified view. *IEEE Trans. Knowledge Data Eng.* 27, 155–169. doi: 10.1109/TKDE.2014.2316512
- Wu, K., Taki, Y., Sato, K., Qi, H., Kawashima, R., and Fukuda, H. (2013). A longitudinal study of structural brain network changes with normal aging. *Front. Hum. Neurosci.* 7:113. doi: 10.3389/fnhum.2013.00113
- Zhang, Y., Brady, M., and Smith, S. (2001). Segmentation of brain mr images through a hidden markov random field model and the expectation maximization algorithm. *IEEE Trans. Med. Imaging* 20, 45–57. doi: 10.1109/42.906424

Conflict of Interest Statement: The authors declare that the research was conducted in the absence of any commercial or financial relationships that could be construed as a potential conflict of interest.

Copyright © 2018 He, Xu, Zhang, Li, Nie, Yap and Shen. This is an open-access article distributed under the terms of the Creative Commons Attribution License (CC BY). The use, distribution or reproduction in other forums is permitted, provided the original author(s) and the copyright owner(s) are credited and that the original publication in this journal is cited, in accordance with accepted academic practice. No use, distribution or reproduction is permitted which does not comply with these terms.